Lasers in Manufacturing Conference 2015

Analysing Hot Crack Formation in Laser Welding of Tempered Steel

Marcel Schaefer[a]*, Nicolai Speker[a], Rudolf Weber[b], Thomas Harrer[a], Thomas Graf[b]

[a]*TRUMPF Laser- und Systemtechnik GmbH, Johann-Maus-Strasse 2, 71254 Ditzingen, Germany*
[b]*Universitaet Stuttgart, Insitut fuer Strahlwerkzeuge (IFSW), Pfaffenwaldring 43, 70569 Stuttgart, Germany*

Abstract

Tempered steel is used in many automotive and aviation parts due to its beneficial material properties such as the combination of high tensile and fatigue strength. Therefore, steel grades like e.g. 42CrMoS4 are used for steering knuckles, axles, connecting rods, drive shafts, pinions, gearwheels, pistons and other highly stressed components (Key to Steel, 2007). Laser welding such parts has the advantage of high welding speed, low heat input, low distortion and high weld seam quality (Huegel and Graf, 2014).
However, seam defects may occur which reduce weld seam strength. In that respect, hot cracks are severe weld defects which are not tolerated, according to ISO 13919-1. In general hot crack formation depends on three factors affecting each other (Cross, 2005): energy deposition into the part (heat input; welding parameters), part design (geometry; restraining conditions) and material properties (solidification temperature range).
To separate the influence of the above-mentioned factors welding experiments were conducted with varying parameters including beam focusing, beam quality and laser power for partial or full penetration depth. Examining the welding process was done by means of 2D x-ray inspection and longitudinal respective transversal cross sections.
In this paper the analysis of continuous crack formation within laser welds in tempered steel will be presented. Additionally, possibilities to reduce and even avoid such severe seam defects will be discussed. Moreover, a new approach of explanation for the formation mechanism of transverse hot cracks will be presented.

Keywords: Tempered steel; laser welding; hot cracks; 2D x-ray inspection; transverse cracks; 42CrMoS4

1. Motivation

Laser welding of high strength steel is a major objective in modern joining operations. Due to its low heat input and low distortion, laser welding is the method of choice especially for rotationally symmetric parts with high requests in runout accuracy. However, hot cracks appear at welding tempered steel like for example 42CrMoS4. Figure 1 shows the cross section and the surface of a transverse crack found in a weld conducted in 42CrMoS4 (1.7227) with 4 mm penetration depth.

* Marcel Schaefer. Tel.: +49-7156-303-31395; fax: +49-7156-303-931395.
E-mail address: Marcel.Schaefer@de.trumpf.com.

Within the cross section depicted in Figure 1 the direction of view for the scanning electron microscope (SEM) picture (b) is marked with a red arrow. Analysis of the crack surface using SEM indicates that solidification cracking takes place in the very last moment of solidification (Zacharia, 1994). However, the local solidus temperature during welding can be significantly lower than the solidus of the alloy valid for very low cooling rates (Zacharia, 1994; Prokhorov, 1962). In Figure 1 (b) a free solidified dendritic structure appears when examining the transverse hot crack – characteristic for the presence of a liquid film lasting until the very end of solidification.

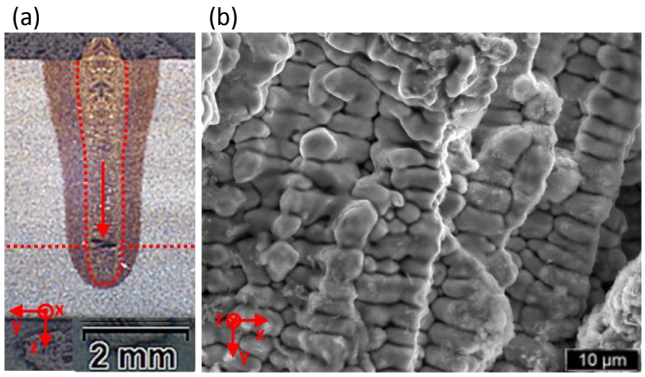

Fig. 1. (a) Cross section of a weld in 42CrMoS4 with showing a transverse crack; (b) classical hot crack surface or solidification crack of the weld of picture (a), direction of view marked with red arrow, showing classic hot cracking with free solidified dendrites.

Stritt (Stritt, 2014) identifies three types of crack initialization theories and summarizes their authors: based on solidification (Borland, 1960), based on strain (e.g. Feurer, 1976) and based on stress (e.g Zacharia, 1993). Stritt combines these three theories in his hot crack susceptibility factor. This hot crack criterion describes the initial phase of a hot crack development as a function of the effective stress and mechanical strain at the solidification front (end of melt bath). Additionally, metallurgical issues are considered through the ratio of solidification volume to melt bath volume. The larger the resulting value multiplying all these factors the higher the susceptibility to hot cracks or solidification cracks.

The behavior of the material in respect of mechanical stress and strain strongly depends onto the heat input. Therefore, the goal of the experiments is to analyze the influence of laser as heat source on the formation of solidification cracks.

2. Experimental

Keeping some restraining conditions the same (e.g. sample design and material) the influence on hot cracks of the laser for welding tempered steel can be analyzed. To separate the influence of the above-mentioned hot crack influencing factors as stated by Cross (Cross, 2005, basic correlations shown in Appendix A.1) welding experiments were conducted using the following parameters:

- Beam focusing: M = 1:1; M = 2.67:1
- Beam quality: BPP = 2 mm·mrad; BPP = 4 mm·mrad; BPP = 16 mm·mrad
- Welding speed: v = const.= 4 m/min (all experiments)
- Penetration depth: s = 5 mm (full penetration); s = 4 mm (partial penetration)

Prior to welding the samples were preheated up to 500°C to prevent cold cracking in the weld due to the formation of martensite. The penetration depth was set by adapting laser power while welding speed was kept constant for all experiments.

Examining the parameter dependent crack susceptibility was done by 2D x-ray analysis. Therefore small pieces with 6 mm in width and 40 mm of length were cut out of the weld sample (150x60x5 mm^3; length of weld l = 120 mm) using a laser cutting machine.

3. Results

3.1. Crack dependency on beam quality and focal position

3.1.1. Welds with transverse cracks

Figure 2 shows x-ray images of the considered alloy (42CrMoS4) (original colors changed from black and white to blue, green and white for better visible crack detection). Parameters for beam quality and focal position of the weld are listed beside each corresponding x-ray picture (left picture) and transversal cross section (right picture). This alloy suffers from hot cracks that are oriented perpendicular to the direction of penetration – so called transverse cracks. These hot cracks extend over several millimeters of the weld seam as indicated by the white stripes and marked with red arrows in the x-ray images in Figure 2. Wherever the cross section hits a transverse crack the crack is marked by a dashed circle around it in Figure 2.

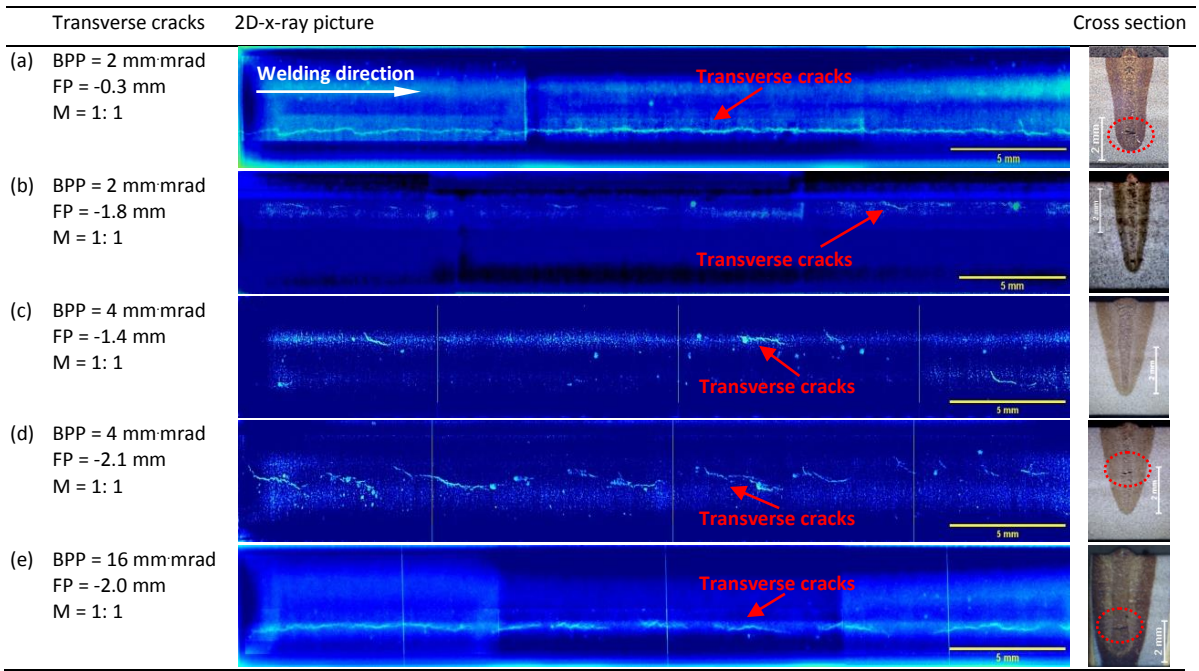

Fig. 2. Comparison of crack formation in welds conducted with different beam qualities and focal positions but same optical magnification (M = 1:1). Transverse cracks (white lines in x-ray picture) are marked in red with dashed circles in the cross section whenever possible.

The crack susceptibility significantly depends on beam quality and focal position. At BPP = 16 mm.mrad an almost continuous crack over 40 mm weld length appears (e). The same is valid for BPP = 2 mm.mrad at focal position FP = -0.3 mm (a). Changing focal position at BPP = 2 mm.mrad to FP = -1.8 mm (b) shifts the crack formation close to the seam surface. Comparable behavior can also be examined at BPP = 4 mm.mrad: While at focal position FP = -1.4 mm there are only few cracks close to the seam surface (c), FP = -2.1 mm leads to a wavy crack formation with few interruptions at approximately half of the penetration depth (d). The comparison between row (d) and row (3) visualizes the influence of beam quality at same focal position. With BPP = 4 mm.mrad (d) the vertical crack position is closer to the seam surface than for the weld carried out with BPP = 16 mm.mrad (e).

3.1.2. Welds without cracks

Cracks reduce weld seam strength especially in case of dynamic load (Schulze, 2010). Therefore, the objective of the experiments was to achieve crack free weld seams. One solution to achieve crack free weld seams is to increase laser power while keeping welding speed the same until full penetration of the weld sample is reached (here full penetration is reached for s = 5 mm).

This approach of full penetration welding to avoid transverse cracks was seen to be valid for all beam qualities: There were no cracks visible in the seams when full penetration is reached. One example of a crack free weld is seen in the longitudinal section and cross section in Figure 3 (a). This weld was carried out using BPP = 16 mm·mrad, an optical magnification of M = 1:1 and adjusted laser power to reach full penetration (s = 5 mm). The left images in Figure 3 are longitudinal sections of 20 mm length in the center of the weld. The position of the longitudinal section is marked with red dashed lines in the corresponding transversal cross section (right picture in Figure 3). The orientation of the weld is illustrated by red Cartesian coordinate systems. Welding direction equals increasing x-axis values. These results being also counterchecked by means of 2D x-ray pictures.

More demanding are crack free welds with partial penetration. It was seen that cracks appeared in any case using an optics with M = 1:1. However, for BPP = 2 mm·mrad and an optical magnification of M = 2.67:1 cracks also disappeared for partial penetration welds – as presented in the longitudinal and transversal cross section in Figure 3 (b).

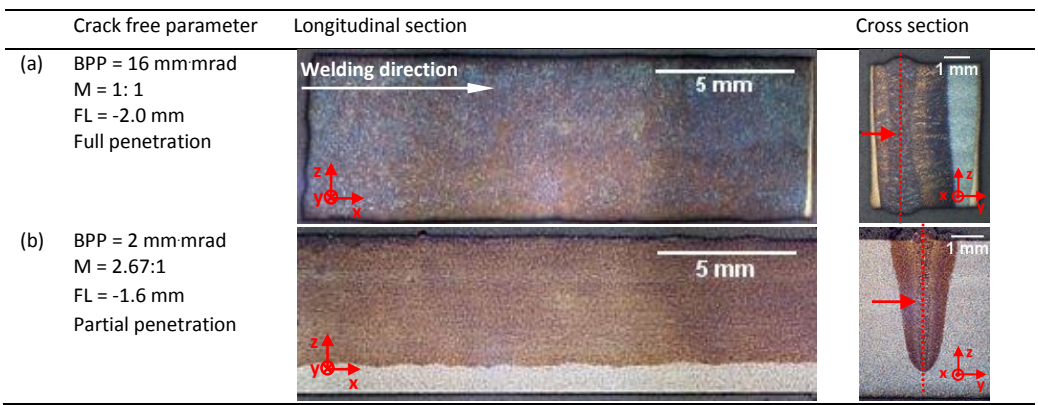

Fig. 3. Crack free weld seams for full penetration at optical magnification of M = 1:1 (a) and for partial penetration at higher optical magnification M = 2.67:1 (b).

Comparing the results of welds with cracks and welds without cracks, the assumption is close that the formation of these cracks has something to do with melt bath dynamics. Therefore, an analysis of melt flow behavior in pictures of the solidified melt was conducted.

3.2. Melt flow behavior

To evaluate the behavior of different welding parameters with respect to the melt flow, bead on plate welds in overlap joint configuration were examined. Therefore, a mild steel plate (1.0037; S235JR; 2.5 mm thick) was put on top of a stainless steel plate (1.4301; X5CrNi-18-10; 2.5 mm thick). Referring to Hess (Hess, 2008) this welding configuration is labeled as “sandwich configuration welds”. To analyze the melt flow behavior longitudinal sections in the middle of the weld seam are prepared by means of etching.

In Figure 4 sandwich configuration welds have been welded using a beam quality of BPP = 4mm·mrad, an optical magnification of M = 1:1 and adopted laser power to reach partial penetration depth of s = 4 mm.

The melt flow behavior differs dramatically when changing focal position as illustrated in Figure 4 in pictures of the solidified melt. The left images show longitudinal sections (10 mm length) of the sandwich configuration weld in which the white dashed lines indicate the thickness of the plates before welding. Welding direction is to the right with partial penetration depth of s = 4 mm. The detailed pictures in second column of Figure 4 (6 mm total length) correspond to the white dashed rectangles in the left overview picture. In the third image of row (a) and (b) in Figure 4 the transversal cross section of these welds is presented. The upper plate is labeled as mild steel. The characteristic appearance of both alloys after etching can be seen beside the weld seam in the cross sections.

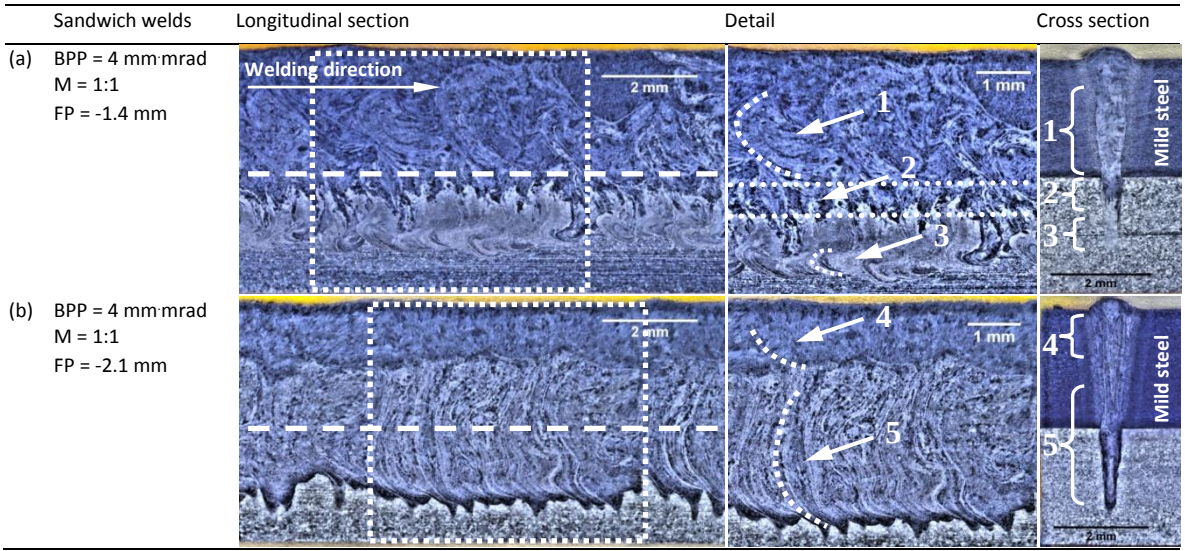

Fig. 4. Sandwich configuration welds (top sheet of mild steel S235JR, bottom sheet of stainless steel X5CrNi-18-10) to visualize melt flow behavior at different focal positions.

At focal position FP = -1.4 mm (a) some amount of the austenitic steel (X5CrNi18-10) is transported to the upper part of the weld where a mixing with ferritic steel (S235JR) takes place. This region of the melt bath is labeled number 1 in the detailed longitudinal section as well as in the cross section. At the lower tip of the melt bath (region 3) no mild steel can be examined, especially in the cross section: There is almost no contrast between the weld and the original material in this region 3 after etching. Between these two regions (region 1 and region 3) an area with local accumulation of mild steel can be examined (dark blue parts in region 2) in the longitudinal as well as in the transversal cross section.

Welding the bead on plate sample with focal position FP = -2.1 mm (b) the resultant longitudinal section looks different: There is no region 3 where only stainless steel is visible at the bottom of the weld. Only the mixing of austenitic and ferritic steel in an area of comparable big extensions at the lower part of the melt bath can be seen (region 5). The dark blue parts indicate that mild steel is transported downwards into the tip of the weld. In melt bath region 4 almost no austenitic steel is visible in the longitudinal section in the middle of the weld seam. However, some of the austenitic steel can be seen at the edges of the weld in the cross section.

4. Conclusion

Welding of tempered steel 42CrMoS4 can cause severe weld defects such as cracks. The analysis of the surface of such cracks using SEM shows free solidified dendritic structures – characteristic for hot cracks. The experiments presented have been carried out to evaluate the hot crack susceptibility in dependence of laser process parameters such as beam focusing, beam quality and penetration depth.

The welds were examined by 2D x-ray analysis as well as longitudinal sections and cross sections of the weld seam. The results show that:

- Hot crack formation in tempered steel strongly depends on beam quality and focal position. For example for BPP = 2 mm·mrad at FL = -1.8 mm only few cracks can be detected while at FL = -0.3 mm continuous formation of a transverse crack appears.
- Crack formation can be avoided when full penetration of the sample thickness is reached. This effect can be seen for all beam qualities and focal positions.
- Cracks in partial penetration welds (s = 4 mm) disappear when higher optical magnification combined with high beam quality (BPP = 2 mm·mrad) is used.

Furthermore, laser welds in sandwich configuration have been done to evaluate the melt flow behavior at different focal positions. At focal position FL = -1.4 mm three melt bath regions can be seen: first, a region at the lower part of the weld where no mild steel can be detected, second, a transition zone where there is an accumulation of mild steel and third, a region of good mixing between mild steel and stainless steel. Changing focal position to FL = -2.1mm the result looks totally different. There are only two melt bath regions where mixing of ferritic and austenitic steel takes place while mild steel is transported into the lowest tip of the melt bath.

Comparing the results of sandwich configuration welds with x-ray inspections of weld seams in tempered steel 42CrMoS4, the assumption can be derived that melt bath dynamics and – to be further examined – melt bath extensions are a factor to consider in case of solidification cracks in laser welds.

Acknowledgements

We like to thank all our colleagues at TRUMPF and at the IFSW who have supported this work. Thanks also to Peter Stritt from the IFSW for fruitful discussions on the topic.

References

Reference book, 2007: Key to steel, Version 5.01.0000 for MS Windows Vista; Verlag Stahlschluessel Wegst, Marbach.

Huegel, H.; Graf, T., 2014: Laser in der Fertigung. Vieweg Teubner Press, 3. Auflage.

International Standard 1996: ISO 13919-1: Electrons and laser beam welded joints, Guidance on quality levels for imperfections – Part 1: Steel (ISO 13919-1: 1996).

Cross, C.E., 2005: On the origin of weld solidification cracking. Hot Cracking Phenomena in Welds, Buch, 394 Seiten, Springer-Verlag, S. 3 - 18.

Zacharia, T., 1994: Dynamic Stresses in Weld Metal Hot Cracking, Welding Journal, 73, p. 164-172.

Stritt, P., 2014: Heißrisskriterium für das randnahe Laserstrahlschweißen von Aluminium. Heißrissbildung beim Laserstrahlschweißen, Workshop – Stuttgart, 18.11.2014.

Borland, J C.: Generalized Theory of Super-Solidus Cracking in Welds (and Castings). British Welding Journal, 8 (1960), 508-512.

Feurer, U., 1976: Mathematisches Modell der Warmrißneigung von binären Aluminiumlegierungen. Gießereiforschung, 2, 75-80.

Zacharia, T.; Aramayo, G. A.: Modeling of Thermal Stresses in Welds. In International Conference on Modeling and Control of Joining Processes, Orlando, Florida.

Schulze, G., 2010: Die Metallurgie des Schweißens. Springer-Verlag, 4. Auflage.

Heß, A; Dausinger, F., 2008: Humping mechanisms during high-speed welding with brilliant lasers. In proceedings of the 3rd Pacific International Conference on Application of Lasers and Optics (PICALO), Beijing, China.

Appendix A.

A.1. Hot cracking theory of Cross

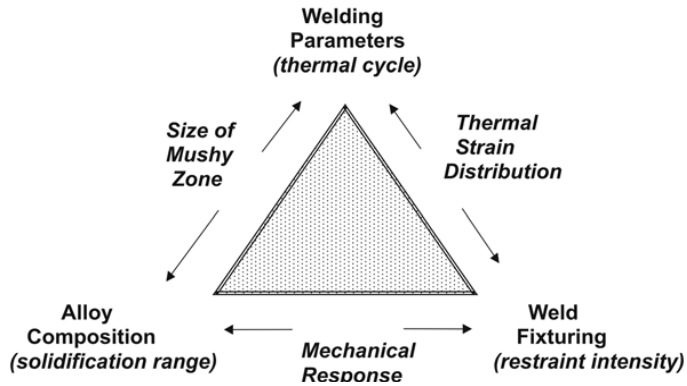

Fig. 5. Diagram indicating interaction between process parameters affecting weld solidification cracking (Cross, 2005).